The Engineering Resource For Advancing Mobility

400 COMMONWEALTH DRIVE WARRENDALE, PA 15096

SAE Technical Paper Series

860535

The Stiller-Smith Mechanism: A Kinematic Analysis

James E. Smith,
Robert P. Craven,
and Robert G. Cutlip
West Virginia Univ.

International Congress and Exposition
Detroit, Michigan
February 24—28, 1986

ISSN 0148-7191

860535

The Stiller-Smith Mechanism: A Kinematic Analysis

James E. Smith,
Robert P. Craven,
and Robert G. Cutlip
West Virginia Univ.

ABSTRACT

The Stiller-Smith Mechanism provides a unique approach in the use of the rotational characteristics of the cross-slider link of the elliptic trammel. Establishment of the research need and a historical development of the design concept are presented complete with a detailed kinematic analysis. Successful incorporation of the new mechanism is pictorially presented.

FOR NEARLY A CENTURY the slider-crank has been the predominant mechanism utilized in the conversion of reciprocating to angular motion. Although several other linkages have been utilized for a variety of motion conversion applications, the internal combustion engine has allowed the slider-crank to become the most popular and successful. One of the major reasons for its success comes from the lack of design constraints on the strength of its components and the flexibility in geometry of the load bearing surfaces and reaction points. A simplified view of the slider-crank reveals a significant weakness in this design due to the characteristic non-sinusoidal nature of the motion. The throw of the connecting rod introduces higher-order vibrational terms that require, for several applications, the incorporation of elaborate and expensive balancers.

Proponents of alternative motion conversion devices, and in particular the Scotch yoke family of mechanisms, cite this vibration characteristic as reason enough to redirect research efforts towards other more "smoothly" operating devices. Clearly, if the only difference between linkage groups was the motion characteristics, then more attention would be paid to the development and incorporation of these other mechanisms. In all probability, the direct result would be a shopping list of useable devices from which to choose. Unfortunately, most of these alternatives have presented other design problems such as higher friction, increased noise, and inadequate wear and strength characteristics from available materials. Thus, the slider-crank rightfully remains the predominant motion conversion mechanism.

A quick historical review of mechanisms indicates few of these alternative motion conversion devices have been truly forgotten. Instead, they have been shelved with hopes of finding future solutions to their respective problems. As new technology is developed (materials, lubricants, manufacturing techniques, etc.) these devices are again reinvestigated to determine if they can serve as a replacement for the slider-crank for specific applications.

With the pressures of today's marketplace, the incentives behind investigating alternative mechanisms have been greatly enhanced by the need to economize and increase efficiency. Any motion conversion device that could reduce the size, profile and weight of the present slider-crank configuration would receive considerable attention. This would be particularly true for the transportation related industries.

One family of candidate mechanisms which has received intermittent but intense attention are the four kinematic inversions of the Scotch yoke; the most popular of these being the double cross-slider (elliptic trammel). The ongoing research, discussed herein, hopes to demonstrate that the elliptic-trammel may yet have a bright future because of its potential, in internal combustion engines, to house multiple cylinders in a small and simple package. In addition to the minimized size, this configuration constrains the rods to non-articulating reciprocation and, for a constant angular output, sinusoidal motion. This last characteristic avoids the dwell and the complex balancing schemes required in

0148-7191/86/0224-0535$02.50

some slider-crank applications.

Several research projects (1-6) have been initiated with the goal of utilizing the double cross-slider configuration and motion characteristics. Most of these have attempted to use yoke rollers or complex slider-cranks to link the sliders. Each has had varying degrees of experimental success, but only a few have made progress in the marketplace. Most of the failures appear to come from problems with efficiency, materials or in some cases from a lack of understanding of the mechanism, its motion and its design limitations.

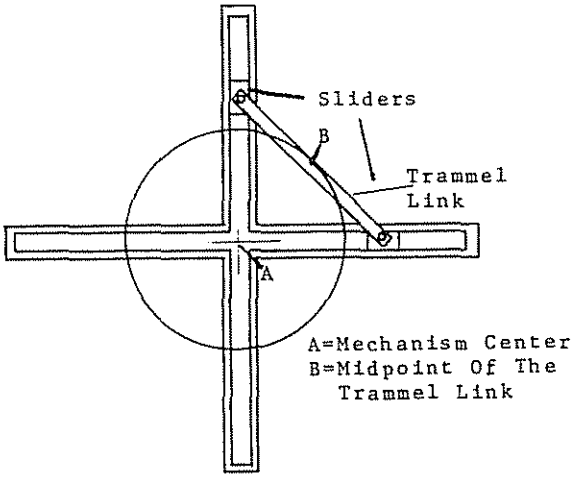

Figure 1. Double Cross-Slider

Figure 1 is a pictorial representation (7) of the four-bar double cross-slider. Each of the two sliders is constrained to move linearly; and they are interconnected by the trammel link. The usefulness of this motion comes as a result of the perpendicular relationship of the two sliders and as a direct consequence of linking the two sliders together by the fixed length of the trammel link (which for an internal combustion engine becomes one-half of the piston stroke). The mid-point of this link, point (B), maps a constant radius circle as the two sliders are forced to reciprocate. Thus, point (B) provides a useful point for power take-off if harnessed properly. Additionally, if the sliders are identical in weight then the mass centers of the sliders and the trammel link can be shown to rotate with point (B), originating from the center of rotation at point (A). Essentially, this acts like a ball on the end of a string and thus balancing, at least theoretically, becomes self-evident. Unexpectedly, as Figure (2) shows, the area around point (B) is not only translating, but is also counter-rotating with respect to the direction of translating point (B). This dual-component of movement provides its own set of problems which have been handled in a variety of ways. With few exceptions, previous linkages incorporate a bearing at point (B) to remove the rotational component of this motion, thus utilizing only the translational component.

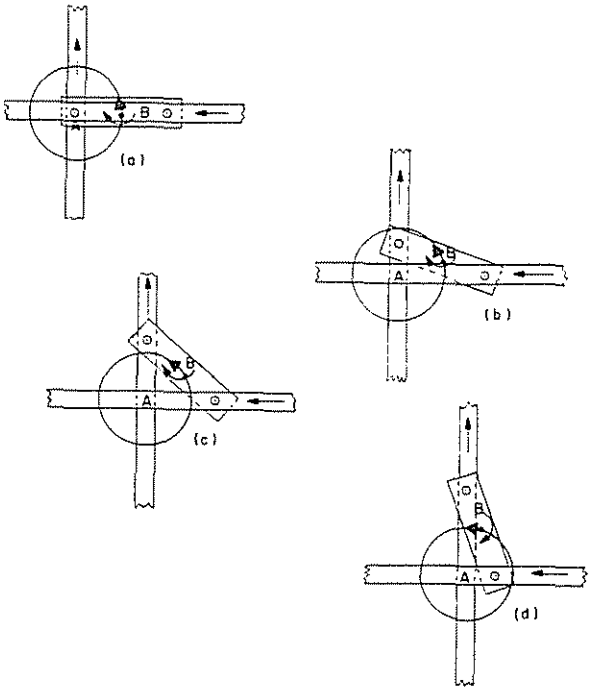

Figure 2. The Double Cross-Slider Motion

It should be noted that the very nature of the double cross-slider isolates the main load bearing components from ground supports and, thus, minimizes the available area for strength considerations. Obviously, if the double cross-slider is to be useful for high load-carrying capacities, such as those associated with internal combustion engines, then a linkage must be incorporated that will take advantage of both the cross-slider configuration as well as the translational/counter-rotational characteristics of the trammel linkage. Additionally, since the trammel link is the main load carrying element in the mechanism and because it is isolated from ground support by the double cross-slider environment, it must be an autonomous force carrying member.

Most of the past research efforts have been quite successful at utilizing the translational characteristics of the trammel motion and some have even provided for first order balancing. Unfortunately, these same efforts have not been able to provide a low friction, durable device that is competitive with the slider-crank mechanism.

One of the initial objectives of the Stiller-Smith Engine Research Project was to investigate unique ways to use the elliptic trammel configuration; the charter being to reduce or eliminate those design limitations that have formerly detracted from the usefulness of the mechanism. The kinematic analysis that follows was a successful attempt to take advantage of the rotational instead of the translational characteristics of the trammel link. For this project the linkage was incorporated into an internal combustion

engine. It was felt that if this new mechanism could function in an engine or pump/compressor environment, then it would generate the required industrial and academic interests necessary to promote adequate research for additional applications of the mechanism.

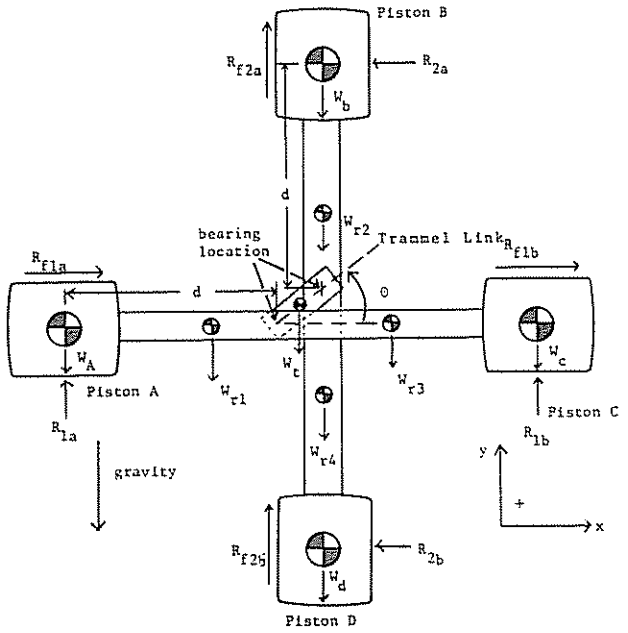

Figure 3. Engine Component Layout Model

The first step in the design of the proposed engine, like any other "motion" device, consisted of a thorough kinematic analysis of the components. Figure 3 is a proposed engine layout where the sliders of Figure 1 are now non-articulating connecting rods of finite length with rigidly attached pistons at both ends. For this analysis the components are assumed to be rigid, the connecting rods are constrained to move linearly and are perpendicular to each other and the motion of the connecting rods are sinusoidal. Also note that this analysis is restricted, for simplicity, to only one quadrant of the mechanism; however, it can be easily demonstrated that the analysis and equations are applicable to all four quadrants.

I. TRAMMEL LINKAGE-KINEMATIC ANALYSIS

For thoroughness, consider a basic kinematic analysis of the elliptic trammel mechanism. Figure 4 illustrates the vectorial representation and orientation.

Using a loop equation (8) to solve for the components of the trammel linkage yields

$$\vec{r}_2 + \vec{r}_3 + \vec{r}_4 = 0 \qquad (I\text{-}1)$$

or

$$r_2 e^{j\theta 2} + r_3 e^{j\theta 3} + r_4 e^{j\theta 4} = 0. \qquad (I\text{-}2)$$

Converting the complex notation and remembering that $j = \sqrt{-1}$ yields

$$r_2 (\cos \theta_2 + j \sin \theta_2) + r_3 (\cos \theta_3 + j \sin \theta_3) + r_4 (\cos \theta_4 + j \sin \theta_4) = 0. \qquad (I\text{-}3)$$

From the problem conditions

$$\theta_2 = 90° \text{ and } \theta_4 = 0°.$$

Therefore,

$$r_2 (\cos^{0} \theta_2 + j \sin^{1} \theta_2) + r_3 (\cos \theta_3 + j \sin \theta_3) + r_4 (\cos^{1} \theta_4 + j \sin^{0} \theta_4) = 0$$

or

$$r_2 j + r_3 (\cos \theta_3 + j \sin \theta_3) + r_4 = 0.$$

Separating this equation into the real and imaginary components yields

$$\text{Real: } r_3 \cos_3 \theta + {}_4 r = 0 \; ; \; r_4 = -r_3 \cos \theta_3 \qquad (I\text{-}4)$$

$$\text{Imag: } r_2 + r_3 \sin \theta_3 = 0 \; ; \; r_2 = -r_3 \sin \theta_3 \qquad (I\text{-}5)$$

and

$$\tan \theta_3 = \frac{r_2}{r_4} . \qquad (I\text{-}6)$$

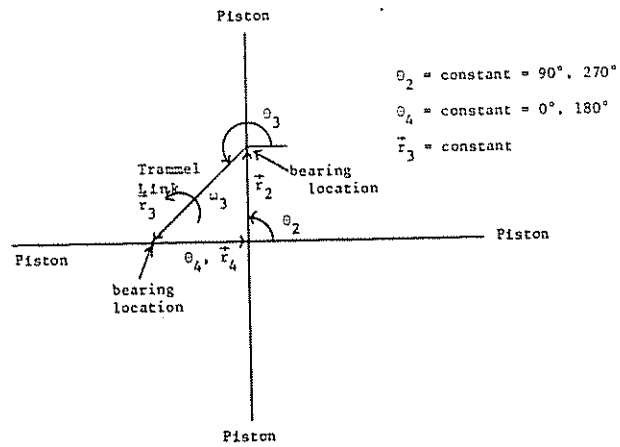

Figure 4. Vector Designation-Elliptic Trammel

Since r_3 and θ_3 are known values, Equations I-4, 5 and 6 can be used with a little manipulation to solve for the positions of each of the pistons with respect to a given trammel angle θ_3. Additionally, differentiation of Equation (I-1) to obtain the velocity equation yields:

$$\dot{r}_4 = r_3\dot{\theta}_3 \sin \theta_3, \qquad \text{(I-7)}$$

$$\dot{r}_2 = -r_3\dot{\theta}_3 \cos \theta_3 \qquad \text{(I-8)}$$

$$\text{and } \tan \theta_3 = -\frac{\dot{r}_4}{\dot{r}_2} . \qquad \text{(I-9)}$$

Since the values of θ_3 and r_3 are known and the angular velocity $\dot{\theta}_3$ is specified for each application, the velocities of each piston can be determined for each position of the piston.

Finally, differentiating (I-1) a second time to obtain the acceleration terms yields:

$$-r_3\ddot{\theta}_3 \sin \theta_3 - r_3\dot{\theta}_3^2 \cos \theta_3 + \ddot{r}_4 = 0 \qquad \text{(I-10)}$$

and

$$\ddot{r}_2 + r_3\ddot{\theta}_3 \cos \theta_3 - r_3 \dot{\theta}_3^2 \sin \theta_3 = 0. \qquad \text{(I-11)}$$

Requiring that $\dot{\theta}_3$, the angular velocity, be constant yields:

$$\ddot{r}_4 = r_3\dot{\theta}_3^2 \cos \theta_3, \qquad \text{(I-12)}$$

$$\ddot{r}_2 = r_3\dot{\theta}_3^2 \sin_3\theta \qquad \text{(I-13)}$$

$$\text{and } \tan \theta_3 = \frac{\ddot{r}_2}{\ddot{r}_4} . \qquad \text{(I-14)}$$

Again, since θ_3 and r_3 and $\dot{\theta}_3$ are known or specified quantities, the acceleration for each of the pistons can be determined for each position and velocity of the piston.

II. CRANK VECTOR-KINEMATIC ANALYSIS

To better understand this mechanism and to put all the parameters in terms of one angular rotation, a special vector was created and designated as the crank vector. This vector originates (Figure 5) at the geometric center of the engine, as a fixed reference to describe the relative motion of the mechanism. Note that the origin of this vector is not positioned on any of the moving parts. It is measured from the center of the engine block to the middle of the trammel link and is constant in length equal to one-half the length of the trammel link or one-quarter the stroke of the piston.

Again, note that this analysis is restricted, for simplicity, to only one quadrant of the mechanism.

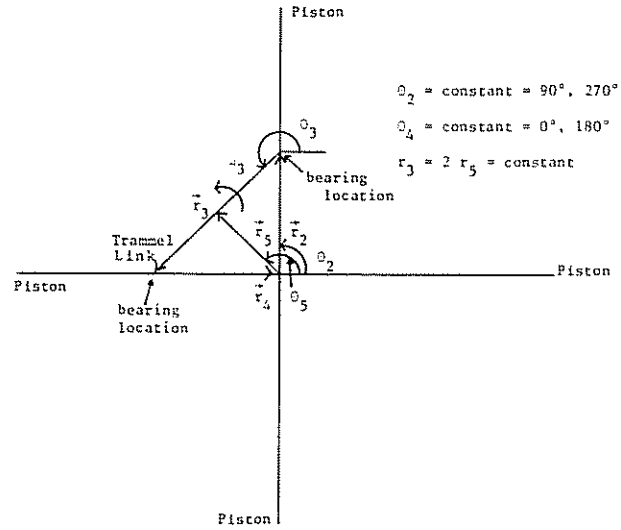

Figure 5. Crank Vector Designation of the Elliptic Trammel Linkage

Using the loop equation for the crank vector

$$\vec{r}_5 + \frac{\vec{r}_3}{2} + \vec{r}_4 = 0 \qquad \text{(II-1)}$$

or

$$\vec{r}_2 + \frac{\vec{r}_3}{2} - \vec{r}_5 = 0. \qquad \text{(II-2)}$$

From Equation (II-1)

$$r_5\, e^{j\theta 5} + \frac{r_3}{2}\, e^{j\theta 3} + r_4\, e^{j\theta 4} = 0.$$

Noting that $\theta_2 = 90°$ and $\theta_4 = 0°$ this equation yields

$$r_5(\cos \theta_5 + j \sin \theta_5) + \frac{r_3}{2} (\cos \theta_3 + j \sin \theta_3)$$

$$+ r_4 (\cos \overset{1}{\cancel{\theta_4}} + j \sin \overset{0}{\cancel{\theta_4}}) = 0.$$

Separating into like components yields

$$\text{Real: } r_5 \cos \theta_5 + \frac{r_3}{2} \cos \theta_3 + r_4 = 0 \qquad \text{(II-3)}$$

and

$$\text{Imag: } r_5 \sin \theta_5 + \frac{r_3}{2} \sin \theta_3 = 0 \qquad \text{(II-4)}$$

From geometry, if vector $\vec{r}_3$, the trammel link,

is fixed in length and $\vec{r}_2$ and $\vec{r}_4$ are constrained to move along the axis, then $\vec{r}_5 = \frac{\vec{r}_3}{2}$ and

$$\sin \theta_5 = -\sin \theta_3. \qquad \text{(II-5)}$$

From the loop equation (II-2), using the same analysis, the results become

$$\cos \theta_3 = \cos \theta_5 \qquad \text{(II-6)}$$

and

$$\tan \theta_5 = -\tan \theta_3 \qquad \text{(II-7)}$$

or $\theta_3 = 2\pi = \theta_5$.

Thus,

$$r_4 = -r_3 \cos \theta_3 = -2 r_5 \cos \theta_5 \qquad \text{(II-8)}$$

and

$$r_2 = r_3 \sin \theta_3 = 2 r_5 \sin \theta_5. \qquad \text{(II-9)}$$

Equations (II-8 and 9) give the positions of the pistons and trammel linkage with respect to a common crank angle θ_5. With an analysis similar to that provided in Section I the velocity and acceleration equations can also be determined. Only the results of this analysis are provided, for the sake of brevity.

The first differentiation of Equation (II-1) yields

$$\dot{\vec{r}}_2 + \frac{\dot{\vec{r}}_3}{2} - \dot{\vec{r}}_5 = 0 \qquad \text{(II-10)}$$

which results with

$$\dot{r}_2 = 2 r_5 \dot{\theta}_5 \cos \theta_5 \qquad \text{(II-11)}$$

and

$$\dot{r}_4 = 2 r_5 \dot{\theta}_5 \sin \theta_5 \qquad \text{(II-12)}$$

$$\text{or } \tan \theta_5 = -\frac{\dot{r}_4}{\dot{r}_2} \text{ where } \dot{\theta}_3 = -\dot{\theta}_5. \qquad \text{(II-13)}$$

The second differentiation of Equation (II-1) yields

$$\ddot{\vec{r}}_2 + \frac{\ddot{\vec{r}}_3}{2} - \ddot{\vec{r}}_5 = 0 \qquad \text{(II-14)}$$

which results with

$$\ddot{r}_4 = -2 r_5 \dot{\theta}_5^2 \cos \theta_5 \qquad \text{(II-15)}$$

and

$$\ddot{r}_2 = -2 r_5 \dot{\theta}_5^2 \sin \theta_5 \qquad \text{(II-16)}$$

$$\text{or } \tan \theta_5 = -\frac{\ddot{r}_2}{\ddot{r}_4}. \qquad \text{(II-17)}$$

With these equations, the position, velocity and acceleration of each component can be found with respect to a specified crank-vector angle, as well as with respect to each other. The need for this vector will become apparent in the following gear analysis.

III. FLOATING GEAR ANALYSIS

As was indicated earlier one of the goals of this research was to take advantage of the rotational characteristics of the trammel linkage as opposed to the translational component. The key is to directly relate what the trammel link (Figure 1) is doing with respect to any fixed set of coordinates.

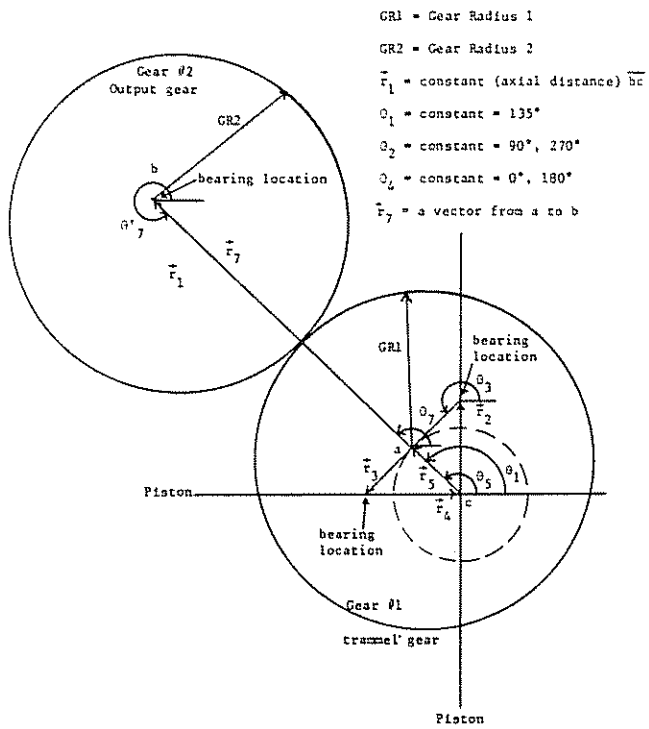

Figure 6. Gear Assembly Vector Designation

The analysis proceeds as follows: First, replace the trammel link by any arbitrary shape. For ease of description call this shape a gear. Second, as a requirement locate another arbitrary shape (output gear) somewhere away from the true center of the engine such that as the gears rotate they maintain constant and uniform contact (Figure 6). Note that because of the offset in the axis of rotation of Gear 1, by the radius r_5 ($r_5 = \frac{1}{4}$ piston stroke), the gears see each other moving in an oscillating fashion first parallel, then either away or toward each other. Since it is a desirable and a practical

engineering requirement, that the motion of the output gear be uniform, it is necessary to design the gears to have solid contact at each point of motion of the trammel gear. Additionally, the output gear should be driven in a way as to approximate, as nearly as possible, constant angular velocity.

The simplest way to design these two gears is to assume that the radius at the point of contact times the angular velocity is equal for each gear, as one would for two stationary gears. Unfortunately, for gears of finite size, this offset and subsequent translation of the axis of Gear 1, introduces measurable error in this assumption. Thus, a different technique must be employed to design these gears. The primary approach in this analysis was to predict the location of the gear contact point and then to evaluate mathematically the precise location (i.e., radius) of each gear with respect to the crank vector.

Consider the vector diagram of Figure 6. Vector $\vec{r}_7$ connects the center of the trammel link and the axial center of the second gear. This vector changes both in size and direction as the position of the crank vector changes. Some moving point on this vector represents a first approximation contact point of the two gears where the sum of Gear Radius 1 and Gear Radius 2 equals the length r_7 at that particular crank angle. As a first approximation, the two gear radii can be assumed to be equal for each crank angle to obtain a set of gear shapes.

From Figure 6 the loop equation becomes

$$\vec{r}_2 + \frac{\vec{r}_3}{2} + \vec{r}_7 - \vec{r}_1 = 0 \qquad \text{(III-1)}$$

or

$$r_2\, e^{j\theta_2} + \frac{r_3}{2}\, e^{j\theta_3} + r_7 e^{j\theta_7} - r_1\, e^{j\theta_1} = 0.$$

But $\theta_2 = 90°$ and $\theta_1 = 135°$ (which was arbitrarily selected for this analysis). Therefore,

$$r_2(\underbrace{\cos\theta_2}_{0} + j\underbrace{\sin\theta_2}_{1}) + \frac{r_3}{2}(\cos\theta_3 + j\sin\theta_3) + r_7(\cos\theta_7 + j\sin\theta_7) - r_1(\underbrace{\cos\theta_1}_{-.707} + j\underbrace{\sin\theta_1}_{+.707}) = 0. \qquad \text{(III-2)}$$

Separating the real from the imaginary terms

$$\text{Real: } 0 + \frac{r_3}{2}\cos\theta_3 + r_7\cos\theta_7 + .707\, r_1 = 0$$

and

$$\text{Imag: } r_2 + \frac{r_3}{2}\sin\theta_3 + r_7\sin\theta_7 - .707\, r_1 = 0.$$

But from Section I, $\sin\theta_3 = -\sin\theta_5$, $\cos\theta_3 = \cos\theta_5$ and $r_2 = 2\, r_5 \sin\theta_5$.

Therefore,

$$\text{Real: } r_5\cos\theta_5 + r_7\cos\theta_7 + .707\, r_1 = 0 \qquad \text{(III-3)}$$

and

$$\text{Imag: } r_5\sin\theta_5 + r_7\sin\theta_7 - .707\, r_1 = 0. \qquad \text{(III-4)}$$

Solving for θ_7 yields

$$\tan\theta_7 = \frac{-r_5\sin\theta_5 + .707\, r_1}{-r_5\cos\theta_5 - .707\, r_1}$$

or

$$\theta_7 = \tan^{-1}\left[\frac{-r_5\sin\theta_5 + .707\, r_1}{-r_5\cos\theta_5 - .707\, r_1}\right]. \qquad \text{(III-5)}$$

Substituting this value of θ_7 into the real component above yields

$$r_7 = \frac{-r_5\cos\theta_5 - .707\, r_1}{\cos\theta_7}$$

or

$$r_7 = \frac{-r_5\cos\theta_5 - .707\, r_1}{\cos\left[\tan^{-1}\left(\frac{-r_5\sin\theta_5 + .707\, r_1}{-r_5\cos\theta_5 - .707\, r_1}\right)\right]}. \qquad \text{(III-6)}$$

These equations indicate that a variety of shapes and configurations can be chosen that will approximate the required mapping of the two gear surfaces. Two constraints limit the shapes of the gears that would be applicable for this design. These are the input/output characteristics and the design/fabrication requirements for the gears.

Firstly, gear shapes could be chosen to maximize any one of several engine requirements. The major concern though is the input/output characteristics. It is important that the power output have as nearly as possible a constant angular velocity. If not, the motion might be such as to limit the usefulness of the design. Secondly, the design of the gears could be a very costly and

time-consuming process. This is especially true if the gears are a combination of complex shapes.

IV. GEAR SHAPE OPTIMIZATION

Section III demonstrated a method of finding a family of approximate gear shapes by fixing a gear contact point versus the crank-vector angle. The rotation of the crank vector yields a series of x-y plots of gear shapes based on user chosen gear layout and radii. Since fabrication was a major concern and because equal gear radii gave results that were the most acceptable, further effort was spent on a more specialized gear model.

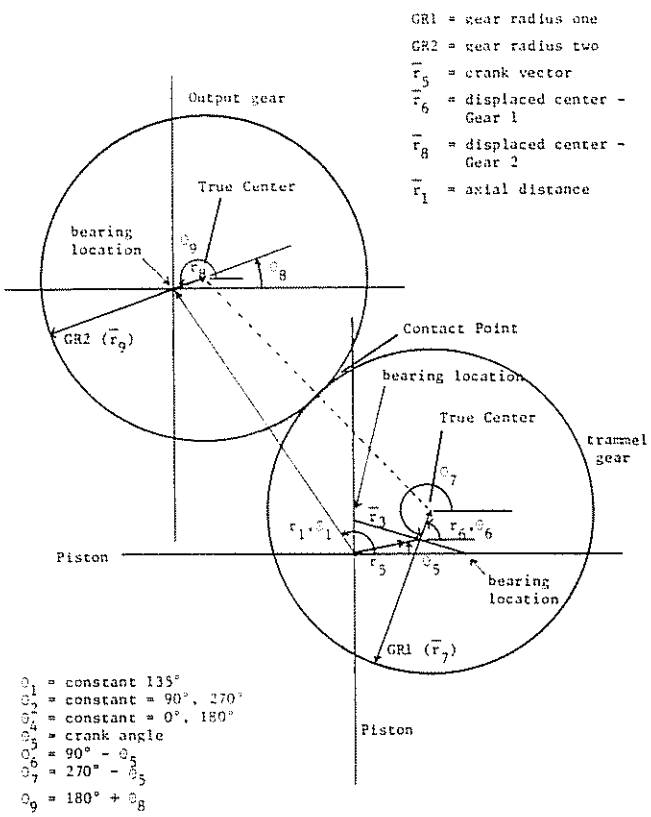

Figure 7. Proposed Equivalent Linkage

Figure 7 represents a vectorial closed loop solution of an equivalent linkage for this design. Note that when comparing this figure with Figure 6 the differences in the results stem from the addition of vectors $\vec{r}_6$ and $\vec{r}_9$. These vectors displace the axial centers and obviously the contact point of the gear teeth.

Vectorially from Figure 7

$$\vec{r}_5 + \vec{r}_6 + \vec{r}_7 = \vec{r}_1 + \vec{r}_8 + \vec{r}_9 \qquad \text{(IV-1)}$$

or

$$r_5 e^{j\theta 5} + r_6 e^{j\theta 6} + r_7 e^{j\theta 7} = r_1 e^{j\theta 1} + r_8 e^{j\theta 8} + r_9 e^{j\theta 9}. \qquad \text{(IV-2)}$$

But the angle that $\vec{r}_6$ makes with respect to $\vec{r}_3$ is fixed and known:

$$\theta_6 = \theta_3 + 90°.$$

Noting that

$$\theta_3 = 360° - \theta_5$$

yields

$$\theta_6 = 90° - \theta_5.$$

With the same manipulations θ_7 can be found with respect to θ_6 or θ_5 and θ_9 can be found with respect to θ_8. With further manipulations the equations yield $\theta_5 = \theta_8$, a most useful relationship.

Or from Equation (IV-2),

$$r_5 e^{j\theta 5} + r_6 e^{j(90°-\theta 5)} + r_7 e^{j(270°-\theta 5)} = r_1 e^{j\theta 1} + r_8 e^{j\theta 8} + r_9 e^{j(180°+\theta 8)}. \qquad \text{(IV-3)}$$

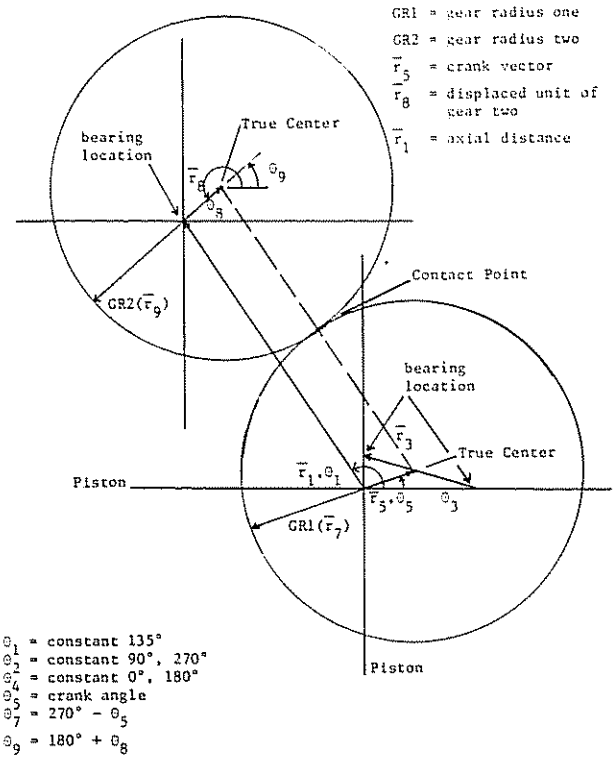

Figure 8. Axial Location for Proposed Gears

By choosing r_1, the axial distance between gears, r_7 and r_9 the gear radii (each equal to 1/2 r_1), and r_5, the crank vector displacement, this equation yields a family of usable solutions, i.e., several of the variables can be changed to provide for a large set of gear centers that will satisfy the required motion. For the engine application covered by this research project, to help with gear balancing, the axial centers were selected to place the true center of the trammel gear exactly between the two axial bearings. This is illustrated in Figure 8. This provides for a better balance of the trammel gear without severely offsetting the axial center of the output gear.

As a last observation, note that because of symmetry several output shafts can be operated from the trammel gear. This is particularly important since a diametrically opposed output gear is fundamental for first-order balancing. This twin output shaft arrangement has been utilized in the most recent working engine prototype illustrated in the summary.

SUMMARY

The enclosed kinematic analysis illustrates another useful option in the utilization of the elliptic trammel mechanism. The use of gears (tooth belts, chains, etc.) with a self-supported floating gear assembly appears to provide a useful and strong energy transfer mechanism (Figure 9).

This linkage has been successfully incorporated into two running prototype internal combustion engines, the latter of which is illustrated by Figure 10. To date, the majority of the research effort has been directed at varifying the above relationships. Future work is now underway to test the effectiveness of the Stiller-Smith Mechanism as a durable and efficient alternative for slider-crank engine applications.

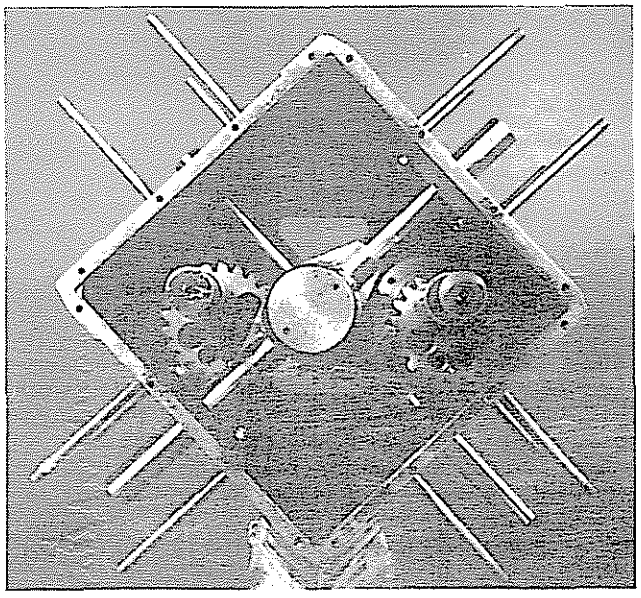

Figure 9. Floating Gear Mechanism of the Stiller-Smith Engine Prototype

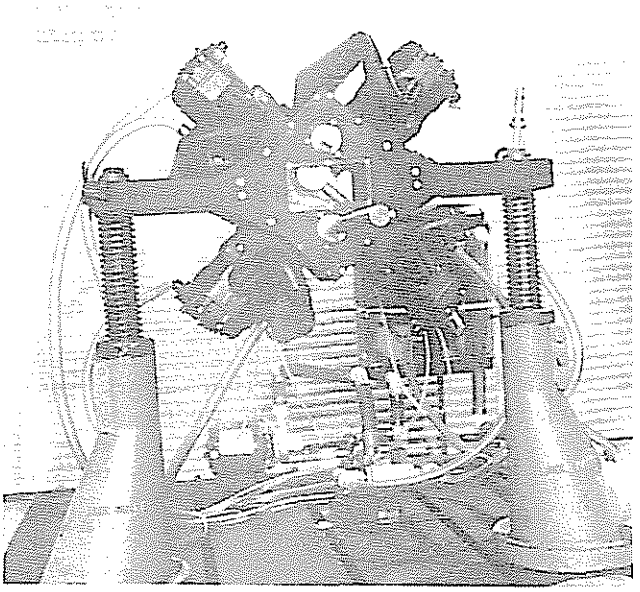

Figure 10. Stiller-Smith Engine Prototype

REFERENCES

1. Hunter, W. J., "Internal Combustion Engine," United States Patent 1181892, May 1916.

2. Bourke, R. L., "Internal Combustion Engine," United States Patent 2122677, July 1938.

3. Reitz, D. M., "Bourke Type Engine," United States Patent 4013048, Mar. 1977.

4. Flinn, Henry L. Jr., "Linear to Rotary Motion Converter Utilizing Reciprocating Pistons," Great Britain Patent 2,038,984, Oct. 1979.

5. Kirk, J. D., "Performance Testing a 30 Cubic Inch Bourke Engine," Sport Aviation Magazine, Mar. 1980.

6. Kirk, J. D., "Design of a Two-Stroke Cycle Spark Ignition Engine Employing a Scotch-Yoke Crankshaft Mechanism," SAE 851518, Sept. 1985.

7. Beyer, Rudolf, The Kinematic Synthesis of Mechanisms, McGraw-Hill Book Co. New York, page 62.

8. Shigley, Joseph Edward and Uicker, John Joseph, Jr. Theory of Machines and Mechanisms, McGraw-Hill Book Co., 1980, page 35.